Taylor & Francis
Taylor & Francis Group

SEPARATION SCIENCE AND TECHNOLOGY

Separation Science and Technology

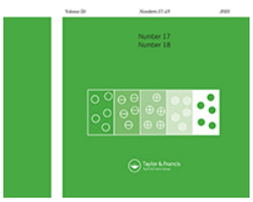

ISSN: (Print) (Online) Journal homepage: www.tandfonline.com/journals/lsst20

Optimization of ultrasound-assisted extraction of galactomannan from carob seeds "*ceratonia siliqua* L" and evaluation of their functional properties and *in vitro* anti-inflammatory activity

Samia Djellal, Farid Dahmoune, Omar Aoun, Hocine Remini, Amine Belbahi, Sofiane Dairi, Hamza Moussa, Mohamed Lakehal, Sabrina Kassouar, Chafika Lakhdari, Meriem Adouane & Nabil Kadri

To cite this article: Samia Djellal, Farid Dahmoune, Omar Aoun, Hocine Remini, Amine Belbahi, Sofiane Dairi, Hamza Moussa, Mohamed Lakehal, Sabrina Kassouar, Chafika Lakhdari, Meriem Adouane & Nabil Kadri (15 Feb 2024): Optimization of ultrasound-assisted extraction of galactomannan from carob seeds "*ceratonia siliqua* L" and evaluation of their functional properties and *in vitro* anti-inflammatory activity, Separation Science and Technology, DOI: 10.1080/01496395.2024.2315608

To link to this article: https://doi.org/10.1080/01496395.2024.2315608

SEPARATION SCIENCE AND TECHNOLOGY
https://doi.org/10.1080/01496395.2024.2315608

Taylor & Francis
Taylor & Francis Group

Optimization of ultrasound-assisted extraction of galactomannan from carob seeds "*ceratonia siliqua* L" and evaluation of their functional properties and *in vitro* anti-inflammatory activity

Samia Djellal[a,b], Farid Dahmoune[b,c], Omar Aoun[c,d], Hocine Remini[b,e], Amine Belbahi[c,d], Sofiane Dairi[c,f], Hamza Moussa[a,b], Mohamed Lakehal[b], Sabrina Kassouar[a,b], Chafika Lakhdari[a,b], Meriem Adouane[a,b], and Nabil Kadri[b,c]

[a]Laboratoire de Gestion et Valorisation des Ressources Naturelles et Assurance Qualité, Faculté des Sciences de la Nature et de la Vie et Sciences de la Terre (LGVRNAQ), Université de Bouira, Bouira, Algeria; [b]Département des Sciences Biologiques, Faculté des Sciences de la Nature et de la Vie et des Sciences de la Terre, Université de Bouira, Bouira, Algeria; [c]Laboratoire de Biochimie, Biophysique, Biomathématiques et Scientométrie (L3BS), Faculté des Sciences de la Nature et de la Vie, Université de Bejaia, Bejaia, Algeria; [d]Department of Microbiology and Biochemistry, Faculty of Sciences, University of M'Sila, M' Sila, Algeria; [e]Centre de Recherche en Technologies Agroalimentaires (CRTAA), Route de Targa Ouzemmour, Campus Universitaire, Bejaia, Algeria; [f]Département de Microbiologie Appliquée et Sciences Alimentaires, Faculté des Sciences de la Nature et de la Vie, Université de Jijel, Jijel, Algeria

ABSTRACT

Ultrasound-assisted extraction (UAE) of galactomannan from the endosperm of ripe carob seeds (LBG.S3) was investigated through response surface methodology (RSM). The optimized UAE conditions were an extraction time of 40 minutes, a temperature of 45°C, and a solid-liquid ratio of 1:50 g/mL. Under these settings, the experimental yield of galactomannan was 47.53 ± 2.55%, which is closely aligning with the expected value of 49.78 ± 3.15%. The yield of galactomannan extracted from unripe carob seeds (LBG.S2) under the same optimal conditions was significantly higher 56.73 ± 2.76% ($p < 0.05$) than the yield of LBG.S3. The infrared spectroscopy (FT-IR) characterization revealed the existence of various functional groups in the spectrum of galactomannan extracted from unripe seeds, not found in LBG.S3. The galactomannan from ripe carob seeds exhibited superior functional properties, including solubility, emulsion and stability capacity, water and oil holding capacity, and viscosity, compared to LBG.S2. *In vitro*, tests demonstrated notable anti-inflammatory activity for both LBG.S2 and LBG.S3, as observed through the inhibition of bovine serum albumin (BSA) protein denaturation by heat and the membrane stabilization test. Carob galactomannan is a potential source of bioactive polysaccharides with anti-inflammatory and functional properties that can be used in the food and pharmaceutical industries.

ARTICLE HISTORY
Received 6 September 2023
Accepted 9 January 2024

KEYWORDS
Ceratonia siliqua seeds; response surface methodology; galactomannan (LBG); anti-inflammatory activity; functional properties

Introduction

The carob tree, scientifically known as "*Ceratonia siliqua* L," is an evergreen species found in the Mediterranean and semiarid regions. It belongs to the Leguminosae family, also known as Fabaceae.[1] This tree is predominantly found in countries such as Portugal, Spain, Italy, Greece, Turkey, Morocco, Algeria, and Tunisia.[2–4] The carob pods have been used for centuries by the populations of the Mediterranean region for the feeding of humans and animals but also they have discovered their therapeutic properties as anti-diarrhea and constipation due to their content of bioactive substances.[5,6] In recent years, their commercial significance has risen significantly, as they are now extensively utilized as raw materials in different industries, including food, cosmetics, and pharmaceuticals.[7]

The pulp represents 90% of the carob pod and is the most frequently used component,[8] serving as the primary raw material for the production of various products, mainly as cocoa substitute.[9] The seeds constitute the remaining 10% and consist of the husk (30–33%), the endosperm (42–46%), and the germ (23–25%).[10] For a long time, carob seeds have been mainly considered as food waste. Nowadays, there has been particular attention toward the recovery of the carob seeds as possible sources of functional compounds with health properties.[11] The main emphasis is on extracting gum from seeds, known under the name of Locust Bean Gum (LBG) or carob bean gum is a water-soluble and neutral polysaccharide called galactomannan, isolated from the endosperm of seeds.[12] These seeds can contain as much as 85% galactomannan content.[10,13] It has been demonstrated that carob seeds are a valuable source not

CONTACT Samia Djellal s.djellal@univ-bouira.dz Laboratoire de Gestion et Valorisation des Ressources Naturelles et Assurance Qualité, Faculté des Sciences de la Nature et de la Vie et Sciences de la Terre (LGVRNAQ), Université de Bouira, Bouira 10000, Algeria

only of phenolic compounds and antioxidants, but also of galactomannan with functional properties that could improve the nutritional value of foods in which are incorporated.[14] Since the 20th century, galactomannans have become industrial products used as a food additive (E410), and in various industries for their many useful properties like thickener, stabilizer, and gelling agent.[15] Chemically, galactomannans are linear polysaccharides,[16] consisting of β-(l-4)-mannose chain sustained by a single D-galactopyranosyl linked via α- (l-6) bonds as a side branch. The main chain does not possess a uniform distribution of these side branches. The degree of substitution by galactose depends on the origin of galactomannans and the extraction conditions.[17]

Carob fruits go through three stages of maturation: the unripe stage (green pods), the semi-ripe stage (green-yellow pods), and the ripe stage (brown pods).[18] The last two stages of maturation are of particular interest for investigation. Ripe carob seeds are well-known for their abundance of galactomannans.[15] However, various studies have shown that the unripe stage of carob, particularly the pulp, possesses significantly higher levels of bioactive compounds and biological activities compared to the mature stage.[19,20] While many polysaccharides derived from natural sources are known for their antioxidant,[21] anti-inflammatory,[22] analgesic,[23] immunomodulatory[24] activities, the biological activities of galactomannan have been poorly studied.[25,26]

The extraction and purification of biomolecules from plants as potential sources of functional compounds with therapeutic effects have become a subject of significant interest.[27] The ultrasound-assisted extraction technique (UAE) is gaining popularity as an environmentally friendly process, utilizing solvents that are generally recognized as safe and reducing processing times. Additionally, it enhances the quality of the bioactive product by yielding higher recovery rates compared to conventional extractions while preserving the extracts' target activities.[28] Furthermore, UAE it can be reduced temperatures with a shorter processing times, leading to energy conservation.[29] Ultrasound consists of mechanical sound waves generated by molecular movements that oscillate within a transmitting medium.[30] The ultrasonic waves create a rapid series of compressions and expansions close to the surface of the solid material. This phenomenon, resembling the repetitive squeezing and releasing of a sponge, is appropriately referred to as the "sponge effect." As a result, tiny channels develop within the material, allowing the solvent to efficiently permeate the solid substance. These channels establish a preferred pathway that facilitates the transfer of dissolved substances from the solid material into the solvent phase.[31–33]

The main goal of this research is the optimization of extraction conditions of galactomannan extracted from carob seeds endosperm using an ultrasound-assisted extraction technique. Once the optimum extraction parameters were honed, a comparative analysis was conducted between the galactomannan obtained from the endosperm of ripe carob seeds and the galactomannan obtained from the endosperm of unripe carob seeds under the same optimal conditions. The study explored the functional properties and the investigated *in vitro* the anti-inflammatory activities of the galactomannan extracted from both ripe and unripe carob seeds. The ultimate aim is to propose a suitable application of this product in various industrial areas.

Materials and methods

Samples

The harvest of carob pods was at the unripe stage in April (the second stage S2 of maturation, because at the first stage of ripening, the seeds are not distinct and we cannot differentiate their different parts: peel, endosperm and embryo) and at the ripe stage (S3) in August,[18] from trees cultivated in the region of M'sila (latitude: N35 ° 44'23'', longitude: E04 ° 33'01 '',' Altitude: 539.00 m Algeria). The samples of carob seeds were removed from the pulp and stored in tightly closed glass jars at a temperature of 4°C in dry and dark environment for the next step.

Reagents

All reagents; Ethanol, Acetone, Sodium dihydrogen phosphate dihydrate (NaH_2PO_4. $2\,H_2O$), Sodium hydrogen phosphate (Na_2HPO_4), Sodium chloride (NaCl), 2-Amino-2-hydroxymethyl-propane-1,3-diol (Tris), and Bovine Serum Albumin (BSA) were purchased from SIGMA-ALDRICH and they were analytical grade.

Extraction procedure

The extraction procedure was conducted in two main steps:

Step 1: Extraction of the raw galactomannan (Endosperm). The seed components were separated following to the procedures presented by Dakia et al.,[10] which involves boiling water pretreatment by immersing carob seeds (100 g) for an hour at 100°C in 800 mL of hot, boiling water. Throughout this pretreatment

procedure, the seeds experience swelling while maintaining the integrity of the seed coat. Subsequently, the seeds are taken out of the water, washed, and the seed coat is manually separated from the endosperm. After being separated from the endosperms, the endosperm is dried at 40°C in an oven until its weight is constant. The endosperms are further processed by grinding using Moulinex (The genuine Type LM241025) and sieved with a 0.125 mm sieve to obtain raw LBG.

Step 2: optimization of UAE conditions and purification of galactomannan. The dry powder of raw carob gum (locust bean gum) underwent extraction with distilled water in an ultrasonic bath (JPSELECTA, sa AC 220 V/240 V.50/60 Hz) with modified extraction conditions (time, temperature, and solid to liquid ratio). The resulting solution and solid phase were separated through centrifugation (SIGMA model 3-16 L Germany) at 8000 g for 10 minutes. The residues were obtained and subjected to extraction by exhaustion ($N = 3$). To purify the LBG, we followed the method described by Bouzouita et al.[13] with slight modification; the LBG extract was precipitated overnight at 4°C with an excess volume of 95% ethanol. The white fibrous precipitate was recovered through centrifugation (8000 g, 10 min) and washed twice with 95% ethanol and acetone. The resulting sediments were collected and lyophilized to reach a constant weight, and the precipitate was subsequently ground into a fine powder. The galactomannan yield (GY (%)) was calculated by the following formula (Equation1):

$$Galactomannan\ Yield(\%) = (M/M_0) \times 100 \quad (1)$$

Where M is weight of the crude extract of water-soluble polysaccharides, and M_0 the weight of dry plant matter (endosperm).[34]

Experimental design

The impact of ultrasonic-assisted extraction (UAE) parameters on the extraction yield of galactomannan from ripe carob seed endosperm was investigated using both full factorial design (FFD) and central composite design (CCD). The FFD was employed to identify the primary extraction parameters significantly affecting galactomannan yield. In contrast, the CCD, utilizing response surface methodology, was used for optimization. Four UAE extraction parameters were considered, including three continuous factors (x_1 : Time, x_2 : Temperature, x_3 : solvent to solid ratio) and one qualitative factor (x_4 : extraction by exhaustion). The range and center point values for these extraction parameters are shown in Table 1. FFD consisted of 19 experimental runs to screen the effect of the four UAE extraction parameters on galactomannan yield (Table 2). Based on the results obtained from FFD, CCD with 17 experimental runs was designed to optimize the galactomannan yield, focusing on the selected parametersx_1 : Time, x_2 : Temperature, x_3 : solvent to solid ratio. The galactomannan yield of was considered as the response, and all results were presented as mean ± SD with triplicates in both Tables 2 and 3. The variables were encoded according to their levels (Table 1) based on their levels (low (−1), median (0), and high levels (+1)), as per equation 2:

$$X = (X_i - X_0)/ \geq X \quad (2)$$

Where X are independent variables at i and 0 levels.

According to the polynomial equation (Equation 3), the experimental data were fitted:

$$\text{galactomannan yield}(\%) = A_0 + \sum_{i=1}^{3} A_i x_i + \sum_{i=1}^{2} \sum_{j=1+1}^{3} A_{ij} x_i x_j + e \quad (3)$$

The galactomannan yield showed a correlation with the three independent variables, as represented by the second-order polynomial equation (Equation 4):

$$\text{galactomannan yield}(\%) = A_0 + \sum_{i=1}^{3} A_i x_i + \sum_{i=1}^{3} A_{ii} x_i^2 + \sum_{i=1}^{2} \sum_{j=1+1}^{3} A_{ij} x_i x_j + e \quad (4)$$

Where A_0 is constant, andA_i,A_{ii} and A_{ij} are coefficients estimated by the model. x_i, x_i^2, $x_i x_j$ are levels of the

Table 1. Coded and real values of inputs variables used for full factorial and central composite design.

	Coded levels				
Factors (Independent variables)	-α	−1	0	+1	+α
x_1 : Time (min)	5.69	10	25	40	44.30
x_2 : Temperature (°C)	13.53	20	42.5	65	71.46
x_3 : solvent to solid ratio (g/mL)	28.46	50	125	200	221.53
x_4 : Extraction by exhaustion($N = 3$)		Yes		No	

(0) represents the center point, (+1, −1) represents the maximum and minimum points, and (-α, α) represents the axial points.

Table 2. Full factorial design (FFD) used for screening the galactomannan yield from the ripe carob seeds.

	Independent variables					
Runs	x_1	x_2	x_3	x_4	Experimental LBG yield (%)	Predicted LBG yield (%)
1	−1	−1	−1	No	5.26 ± 1.68	5.65
2	−1	−1	−1	Yes	11.33 ± 0.42	9.39
3	−1	−1	+1	No	4.8 ± 1.40	5.65
4	−1	−1	+1	Yes	8.86 ± 0.70	9.39
5	−1	+1	−1	No	14.66 ± 0.70	12.93
6	−1	+1	−1	Yes	35 ± 1.44	30.71
7	−1	+1	+1	No	12.33 ± 1.40	12.93
8	−1	+1	+1	Yes	25.46 ± 1.01	30.71
9	+1	−1	−1	No	4.7 ± 1.25	4.51
10	+1	−1	−1	Yes	15.2 ± 0.60	15.95
11	+1	−1	+1	No	5.46 ± 0.42	4.51
12	+1	−1	+1	Yes	15.73 ± 1.80	15.95
13	+1	+1	−1	No	19.8 ± 0.92	19.62
14	+1	+1	−1	Yes	49.2 ± 2.80	45.10
15	+1	+1	+1	No	18.2 ± 0.21	19.62
16	+1	+1	+1	Yes	42.4 ± 0.35	45.10
17	0	0	0	No	10.8 ± 0.90	10.68
18	0	0	0	No	10.8 ± 0.20	10.68
19	0	0	0	Yes	24.46 ± 1.67	25.29

Table 3. Central composite design used for optimization the galactomannan yield from the ripe carob seeds.

	Independent variables			Experimental LBG	
Runs	x_1	x_2	x_3	yield (%)	Predicted LBG yield (%)
1	- α	0	0	14.06 ± 1.01	15.69
2	−1	−1	−1	11.4 ± 0.40	11.99
3	−1	−1	+1	18.6 ± 0.40	16.81
4	−1	+1	−1	28.4 ± 0.53	27.05
5	−1	+1	+1	31.2 ± 0.72	31.62
6	0	- α	0	12.66 ± 0.58	12.94
7	0	0	-α	23.8 ± 0.26	23.38
8	0	0	0	22.16 ± 0.58	21.66
9	0	0	0	21.66 ± 0.76	21.66
10	0	0	0	21.33 ± 1.04	21.66
11	0	0	+ α	23.6 ± 0.53	24.14
12	0	+ α	0	42.83 ± 1.04	42.68
13	+1	−1	−1	18.86 ± 0.83	18.39
14	+1	−1	+1	13.733 ± 1.22	15.02
15	+1	+1	−1	48.05 ± 0.67	49.78
16	+1	+1	+1	46.8 ± 0.23	46.15
17	+ α	0	0	30.66 ± 0.58	29.16

extraction parameters, which represent the linear, quadratic, and cross-product effects respectively, e is the error.

To perform the screening design and RSM experimental design, JMP® software (Version 13) was utilized. The software was also employed to create 3D graphical models for variable responses and predict optimal values for galactomannan yields. Each measurement was performed three times ($n = 3$), and the findings were presented as means and corresponding standard deviations.

Functional properties

Solubility kinetics

The method recommended by Dakia et al.[10] was used to study the solubility kinetics of galactomannan at both 25°C and 80°C. At 25°C (ambient temperature) for 0.5, 1, 2, and 3 hours with stirring, purified LBG powder from LBG.S2 and LBG.S3 was prepared with a concentration of 0.1% (w/w) by dry weight. Other preparations were also made with the same concentration but were heated up for 5, 10, 30, and 60 minutes at 80°C. The appropriate solution was extracted after the allotted time had passed, and then centrifuged (6000 g, 30 minutes, and 20°C) to remove any insoluble material. Based on the total solids dried in an oven for 24 hours at 105°C, the retrieved supernatant and the final polymer concentrations were calculated according to (Equation 5).

$$Solubility(\%) = (Supernatant\ concentration/Initial\ preparation\ concentration) \times 100 \quad (5)$$

Emulsion properties

The two galactomannan samples (LBG.S2 and LBG.S3) were subjected to an analysis of the emulsion stability

(ES) and emulsion capacity (EC). the technique described by Wang et al.[35] was used. At room temperature, three milliliters (3 mL) of sunflower oil were added to ten milliliters (10 mL) of LBG solutions at a concentration of 1% (w/v). A vortex was used to homogenize the mixture for 1 minute, and it was then centrifuged at 1000 g for 10 minutes.

The calculation of the EC was performed using the following equation (Equation 6):

$$EC(\%) = \frac{\text{Emulsion volume}}{\text{Total volume}} \times 100 \quad (6)$$

The emulsion was heated for 30 minutes at 80°C, cooled to room temperature, and then centrifuged at 1000 g for 10 minutes to determine the ES. The following equation (Equation 7) was applied to calculate the ES:

$$ES(\%) = \frac{\text{Final emulsion volume}}{\text{Total volume}} \times 100 \quad (7)$$

Water holding capacity (WHC) and oil holding capacity (OHC)

To determine these parameters, we adopted the method recommended by Niknam et al..[36] Initially, 0.4 g of purified LBG powder (LBG.S2 and LBG.S3) was precisely measured. The samples were then gradually added 40 mL of either sunflower oil or distilled water. The solutions were shaken intermittently every five minutes for about an hour at room temperature. The solutions were centrifuged at 3000 g for 30 minutes after the specified time had passed. The residue was weighed to determine the WHC and OHC, which represent, respectively, the percentage of water or oil retained per gram of the sample.

Viscosity

The viscosity of galactomannan (LBG.S2 and LBG.S3) was assessed using a Falling Ball Viscometer C (Thermo Scientific™ HAAKE™) following the methodology outlined by Bostanudin et al..[37] Distilled water was used to dissolve the samples at a concentration of 0.1%. The viscometer's constant was 0.007mPa·s·cm^3/g.s, and the glass ball (boron silica glass) had a density of 2.2 g/cm^3, while the liquid had a density of 0.1 g/cm^3. To assess viscosity, a polysaccharide solution of around 45 cm^3 was poured into the measuring tube, filling it up to 20 mm below the rim. Subsequently, the ball was gently added to the solution and allowed to fall. After that, it was noted how long it took for the ball to pass through the sample solution. The dynamic viscosity η (in mPa·s) of galactomannan was calculated using Equation 8:

$$\eta = K(\rho 1 - \rho 2) \times t \quad (8)$$

Where ρ1 represents the density of the ball in g/cm^3; ρ2 the density of the liquid in g/cm^3; t the falling time of the ball in the liquid (measured in seconds); K the Ball constant in mPa s cm^3/g s.

Fourier-transform infrared spectroscopy (FT-IR) analysis

Purified galactomannan (LBG.S2 and LBG.S3) was analyzed for major structural groups using a JASCO FT/IR-4200 infrared spectrometer with ATR PRO450-S mode. Spectra were scanned in the range of 7800 to 350 cm^{-1}.

Anti-inflammatory activity

Inhibition of bovine serum albumin protein denaturation

According to Lekouaghet, Boutefnouchet,[38] the bovine serum albumin (BSA) protein denaturation test was applied to assess the *in vitro* anti-inflammatory activity of galactomannan (LBG.S2 and LBG.S3). The extract was mixed with 0.5 mL of BSA solution (0.2%) prepared in Tris buffer (pH 6.6) for each concentration of the extract (50, 100, 200, 400, 600, 800, and 1000 g/mL). The samples were then incubated for 15 minutes at 37°C in the oven, then for 5 minutes at 72°C in a water bath. After the tubes had cooled, the turbidity (amount of protein precipitation) was assessed at 660 nm with a spectrophotometer, and Equation 9 was used to determine the percentage inhibition of protein denaturation:

$$\%\ inhibition = (Abs\ of\ the\ control - Abs\ of\ the\ treated\ sample)/Abs\ of\ the\ control \times 100 \quad (9)$$

The control sample corresponds to 100% of the denatured proteins.

Membrane stabilization test

The hemolysis or membrane stabilization activity induced by the hypotonic solution was determined using the method outlined by Shinde et al..[39]

Erythrocyte suspension. A healthy human participant who had abstained from taking nonsteroidal anti-inflammatory medicines for two weeks before to the trial provided the blood that was used in the experiment. After that, the blood was put in a heparinized tube and washed three times in a 0.9% saline solution. An isotonic buffer solution (pH 7.4) containing 1 L of distilled water, 0.26 g of NaH2PO4, 1.15 g of Na2HPO4, and 9 g of NaCl (10 mM sodium phosphate buffer) was used to

reconstitute the measured volume of saline solution into a 40% (v/v) suspension.

Hemolysis induced by hypotonic solution. The isotonic buffer solution was prepared by combining 154 mM NaCl with 10 mM sodium phosphate buffer at pH 7.4. The experiments were conducted in triplicate. The hypotonic solution, containing galactomannan preparations (LBG.S2 and LBG.S3) at concentrations of 50, 100, 200, 400, 600, 800, and 1000 g/mL, was mixed with a stock suspension of 30 µL erythrocytes. As a control, the hypotonic-buffered solution was mixed with 30 µL of erythrocyte suspension. Following a 10-minute incubation at standard room temperature, the mixtures were centrifuged at 1300 g for 3 minutes. The absorbance of the supernatant was determined at 540 nm. The percentage inhibition of hemolysis was calculated using Equation10:

$$\%inhibition\ of\ hemolysis = (Absofcontrol - Absoftest)/ Absofcontrol \times 100 \quad (10)$$

Statistical analysis

The data was analyzed using Graph Pad Prism Software (Version 8), which were then presented as mean SD. For the statistical analysis, one-way or two-way ANOVA was applied, with a significance level of $p \leq 0.05$. Each analysis was carried out three times.

Results and discussion

Preliminary study

Fitting the FFD model

The FFD model for galactomannan yield was evaluated by applying the analysis of variance (ANOVA), lack of fit (LOF), *R*-squared (R^2), adjusted *R*-squared (R^2_{Adj}), and coefficient of variation (CV %). The obtained results showed a good fit with an R^2 value of 0.98, indicating that 98% of the data fit the adjusted regression model. The CV value was 12.42% (Table 4), which further supports the accuracy of the model. Moreover, the higher adjusted *R*-square ($R^2_{Adj} = 0.97$) indicated that 97% of the variation in galactomannan yield can be explained by the UAE extraction parameters that significantly affected the response. The ANOVA results (Table 4) showed that the mean response values are significantly different. (greater F-value, with $p < 0.05$), and the lack of fit was not significant (F-value was lower, and $p > 0.05$), indicating a good relationship between the experimental and predicted values of the responses. Thus, the FFD model demonstrated high accuracy and effectively accounted for a significant portion of the response variations.

Effect of the process variables on galactomannan yield (GY)

In this study, a four-factor, two-level FFD was employed to screen the major extraction parameters that affect galactomannan yields. The extraction time, extraction temperature, solid-liquid ratio, and extraction by exhaustion ($N = 3$) were the independent variables considered in the ultrasonic-assisted extraction (UAE) of polysaccharides from carob seed endosperm. By contrasting the estimated coefficients, a polynomial equation was established to evaluate the impact of the factors (independent variables). The regression model for galactomannan yield (GY%) is illustrated by equation (Equation 11).

$$GY(\%) = 17.98 + 3.31x_1 + 9.10x_2 - 1.36x_3 - 7.30x_4 - 3.51x_2x_4 1.92 - 3.51x_1x_4 + e \quad (11)$$

Based on the results from Tables 2 and 4, and Equation 11, it was observed that the extraction time (x_1) had a positive linear impact on the galactomannan yield. This suggests that the duration of extraction influences the efficiency and selectivity of the extraction process. The extended extraction time allows the raw LBG to be in contact with the release medium, facilitating the dissolution of galactomannan from the dried material and its subsequent diffusion into the liquid. Consequently, a longer extraction time positively affects the polysaccharide yield. This finding is consistent with previous studies that have reported that prolonged extraction periods enhance the release of polysaccharides.[40–42]

Table 4. Results of regression coefficients analysis of the predicted polynomial model FFD.

	UAE settings	Estimated coefficient	*P*-value
Estimated parameters	Intercept	17.98	<0.0001[a]
	x_2	9.10	<0.0001[a]
	$x_4[-1]$	−7.30	<0.0001[a]
	x_1	3.31	<0.0001[a]
	x_3	−1.36	0.0293[a]
	$x_2x_4[-1]$	−3.51	<0.0001[a]
	x_2x_1	1.95	0.0043[a]
	$x_4[-1]x_1$	−1.92	0.0048[a]
Regression results	R^2	0.98	
	R^2_{Adj}	0.97	
	RMSE	2.18	
	CV (%)	12.42	
	ANOVA (Model)	$p < 0.0001$[a]	
	Lack of fit	/	

(a) Highly significant, (b) significant, ($p > 0.05$) not significant.

Moreover, the extraction temperature (x_2) also had a significant positive linear effect on the polysaccharide yield, as shown in Tables 2 and 4. This effect was noted within the temperature scale of 20 to 65°C. The obtained result can be attributed to two main physical processes in ultrasound-assisted extraction (UAE): acoustic cavitation and diffusion through cell walls.[43] The extraction temperature plays a significant role in enhancing both of these phenomena, leading to an increase in polysaccharide yield with higher temperatures. However, it is worth noting that excessively high temperatures can have adverse effects on the extraction process. At such elevated temperatures, the surface tension decreases, and the vapor pressure within microbubbles increases, causing the ultrasonic wave to be dampened.[44] Furthermore, elevated temperatures result in reduced viscosity and density of the extracts, facilitating deeper penetration of the solvent into the sample matrix.[45] As the solvent penetrates more deeply, its exposure area expands, leading to greater extraction efficiency. Overall, the optimal extraction temperature should be carefully considered to balance the positive effects on extraction efficiency with the potential negative impact of ultrasonic wave damping at extremely high temperatures.

The impact of the solid-liquid ratio (x_3) on polysaccharide yield was found to be positive at a ratio of 1:50 g/mL. However, with further increases in the ratio, the effect became notably negative in linear terms. A higher solid-liquid ratio led to a more significant concentration difference between the interior plant cells and the external solvent, which in turn facilitated faster diffusion of polysaccharides.[43] However, an excessively high solid-liquid ratio led to an increased diffusion distance within the internal tissues, leading to a slower increase in extraction efficiency as the ratio increased.[45]

Regarding the fourth factor (x_4), conducting the extraction by exhaustion three times proved to be highly effective, resulting in a significant increase in the extraction yield (53.57%). This finding aligns with previous scientific findings that support the notion that repeating the extraction cycle enhances polysaccharide yield.[46–48] However, it should be noted that the method of exhaustion and repeating extraction cycles may involve using a large volume of solvent and increasing the sample processing time, which could potentially lead to sample degradation.[49]

Fitting the CCD model

The CCD model fitting results for galactomannan yields (Table 5) are crucial to evaluate the precision of the model in predicting optimal variations and establishing correlations between the selected parameters of EAU and extraction yield. To assess the reliability and accuracy of the CCD model, an analysis of variance (ANOVA) was conducted. The galactomannan yields obtained from all experiments with predicted values are presented in Table 3. The determination coefficient (R^2) and adjusted R-square (R^2_{Adj}) for galactomannan yields were found to be 0.98 and 0.97, respectively, indicating a strong correlation between actual and predicted values of galactomannan yields. The lack of fit value was assessed to determine the adequacy of the model and was found to be non-significant ($p > 0.05$), suggesting that the model adequately fits the experimental data (Table 3). Furthermore, the coefficient of variance (CV %) was lower than 15%, indicating the adequacy of the CCD model. A second-order polynomial equation (Equation12) was derived through multiple regression analysis on the experimental data to establish the relationship between GY (%) and the test variables.

$$\begin{aligned} GY(\%) = {} & 21.66 + 5.23x_1 + 11.55x_2 + 0.29x_3 + 0.46x_1^2 \\ & + 3.71x_2^2 + 1.26x_3^2 + 4.08x_1x_2 - 2.04x_1x_3 \\ & - 0.06x_2x_3 + e \end{aligned} \tag{12}$$

Table 5. Results of regression coefficients analysis of the predicted quadratic polynomial model CCD.

	UAE settings	Estimated coefficient	*P*-value
Estimated paramaters	Intercept	21.66	<.0.0001[a]
	x_1	5.23	<.0.0001[a]
	x_2	11.55	<.0.0001[a]
	x_3	0.29	0.5381[b]
	x_1x_2	4.08	0.0001[a]
	x_1x_3	−2.04	0.0071[a]
	x_2x_3	−0.06	0.9091[b]
	x_1^2	0.46	0.4910[b]
	x_2^2	3.71	0.0006[a]
	x_3^2	1.266	0.0865[b]
Regression results	R^2	0.992077	
	R^2_{Adj}	0.981891	
	RMSE	1.542932	
	CV (%)	6.05	
	ANOVA (Model)	$p < 0.0001$	
	Lack of fit	0.0520	

(a) Highly significant, (b) significant, ($p > 0.05$) not significant.

Optimization of galactomannan extraction conditions

In this research, a three-factor at three-levels Central Composite Design (CCD) was employed to examine the impact of extraction process variables, namely extraction time, extraction temperature, and solid-liquid ratio, on the ultrasonic-assisted extraction (UAE) yield of galactomannan from carob seeds endosperm. The CCD model allowed the construction of three-dimensional response surface plots (Figure 1) to visualize the main and interactive effects of these independent variables on galactomannan yield (GY%).

In Figure 1a, the response surface plot demonstrates the mutual interaction between extraction time and temperature on galactomannan extraction yield while keeping the solid-liquid ratio constant at its central level. The two variables were altered within their experimental ranges for this analysis.

The 3-D plot demonstrates that as the extraction time increases from 5 to 45 minutes and the extraction temperature rises from 10 to 70°C, the galactomannan extraction yield also increases. Notably, the combined effect of extraction time and temperature (x_1x_2) on the yield is positive and significant ($p < 0.0001$), which is further supported by the regression model coefficients presented in Table 5. Among the factors, extraction temperature exerts the most influential positive linear effect ($p < 0.0001$) on GY (%).

In Figure 1b, the impact of two variables, extraction time and solid-liquid ratio, was investigated while keeping the temperature constant, on the galactomannan yield (GY %). The 3-D plot reveals that the galactomannan extraction yield increases noticeably as both extraction time and solid-liquid ratio increase from 1:50 to 1:200 g/mL. However, beyond the solid-liquid ratio of 1:50 g/mL, the galactomannan extraction yield starts to decrease slowly. The interaction effect between extraction time and the solid-liquid ratio (x_1x_3) on the yield is found to be significant ($p < 0.05$) in a negative way, while the solid-liquid ratio shows a non-significant linear effect ($p > 0.05$) in a positive way on the yield, as indicated in Table 5.

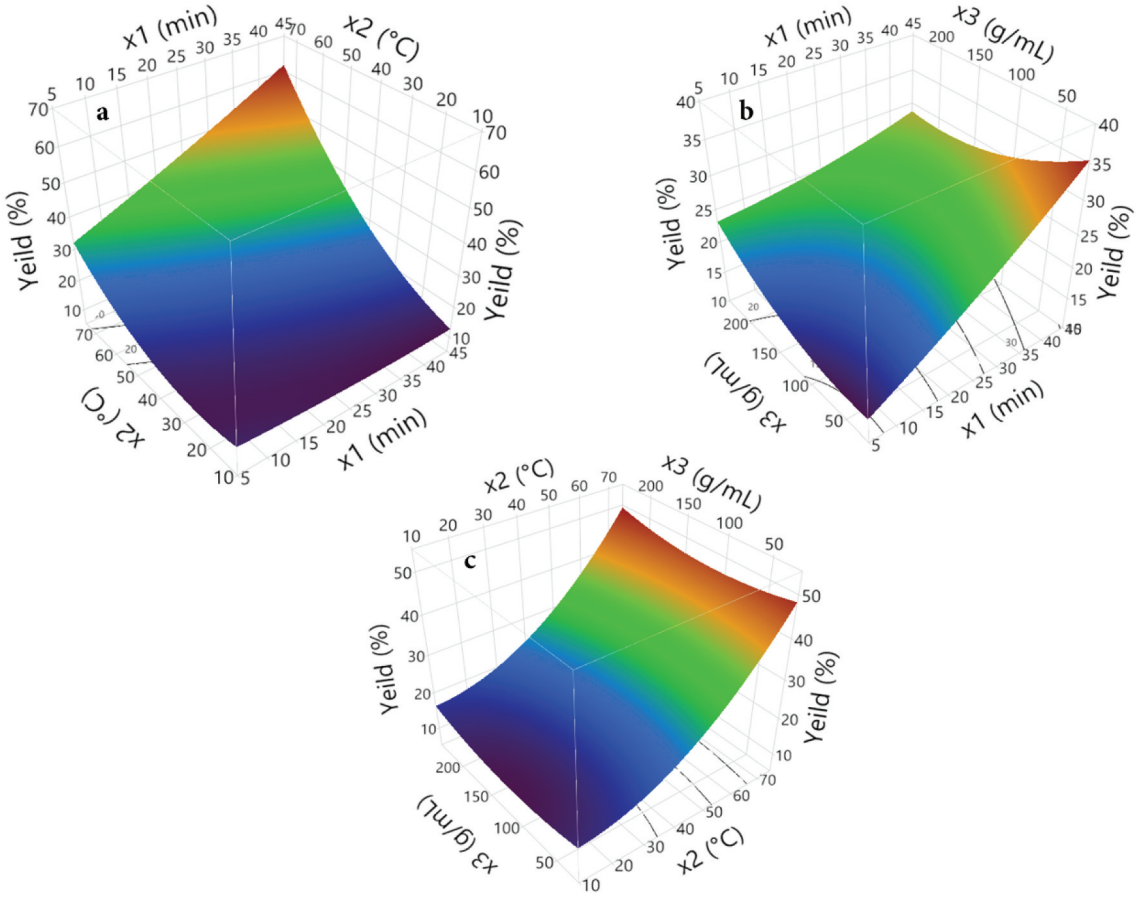

Figure 1. 3D-surface plots CCD using polynomial equations: (a) interactive effect of time and temperature on the extraction of polysaccharides, (b) interactive effect of time and solvent to solid ratio on the extraction of polysaccharides, (c) interactive effect of temperature and solid to solvent ratio on the extraction of polysaccharides.

Furthermore, according to the results presented in Table 5 and Figure 1c, when examining the interaction effect of temperature and solid-liquid ratio (x_2 x_3) while keeping the extraction time fixed at its central value, the percentage of galactomannan yield was not significantly affected ($p > 0.05$) in a negative way. However, the extraction temperature exhibited a significant linear effect ($p < 0.05$) in a positive way on the yield.

Validation of the model

To assess the accuracy of the CCD model equations and validate the optimal extraction conditions ($t = 40$ min, $T = 65$°C, solid-liquid ratio 1:50 g/mL, extraction by exhaustion ($N = 3$)), the model predicted a maximum response of (49.78 ± 3.15%). To ensure that this value aligns well with practical results, a new experimental verification was conducted under the same optimal conditions, yielding an average value of (47.53 ± 2.55%). The close agreement between the predicted and experimental values confirms the validity of the RSM model.

Comparison of extraction yields of galactomannan from the endosperm of ripe (LBG.S3) and unripe (LBG.S2) carob seeds

The extraction and purification of galactomannan from unripe carob seeds (LBG.S2) under the same optimal conditions as ripe carob seeds (LBG.S3) resulted in a higher yield of LBG.S2 at 56.73 ± 2.76%, which was significantly larger ($p < 0.05$) than the yield of LBG.S3 (47.53 ± 2.55%). This difference in yield can be attributed to the stage of maturation during harvest. Previous research by Liu et al.[50] demonstrated that the Mannose/Galactose (M/G) ratio of galactomannan in *Gleditsia sinensis* Lam fruits increased and then decreased with fruit ripening. This suggests that during primary biosynthesis, the galactomannan backbone is initially fully substituted, and some galactosyl groups are later removed by α-galactosidase in the endosperm. These changes may explain the variation in extraction yields between LBG.S2 and LBG.S3.

extracted by UAE exhibited higher yields compared to galactomannans extracted by conventional method (water bath extraction at 80°C), as reported by Bouzouita et al.[13] (26.7 to 33.2% from different carob tree populations in Tunisia), as well as from other seeds such as *Parkinsonia aculeate* (37.8%)[51] and *Trigonella foenum-graecum* (Fenugreek) Seeds (18.54%).[36] The differences in extraction yield values can be attributed to various factors, including the extraction methods, time, temperature, water-to-feedstock ratio, grating step, and environmental conditions.[52]

Functional properties

Solubility kinetics

The solubility kinetics of LBG.S2 and LBG.S3 were examined at 25°C and 80°C (Figures 2 and 3). Initially, both samples exhibited partial solubility at 25°C within the first 30 minutes, followed by a proportional increase over time. Significantly ($p < 0.05$), LBG.S2 achieved 85.70 ± 0.34% solubility after two hours, while LBG.S3 reached 49.79 ± 0.66% at the same time. After three hours, the solubility rates were 85.80 ± 0.69% for LBG.

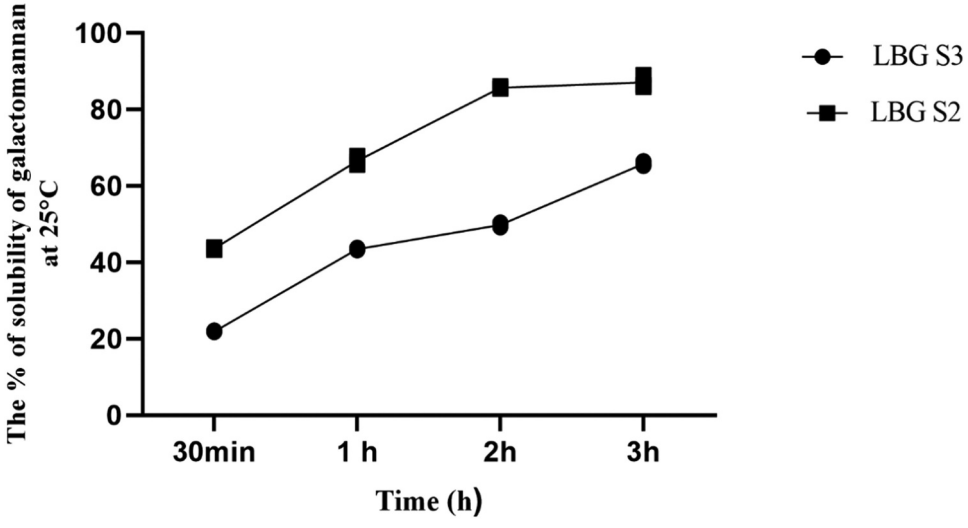

Figure 2. The solubility kinetics at 25°C of galactomannan from the endosperm of the unripe stage (LBG.S2) and ripe stage (LBG.S3) carob seeds.

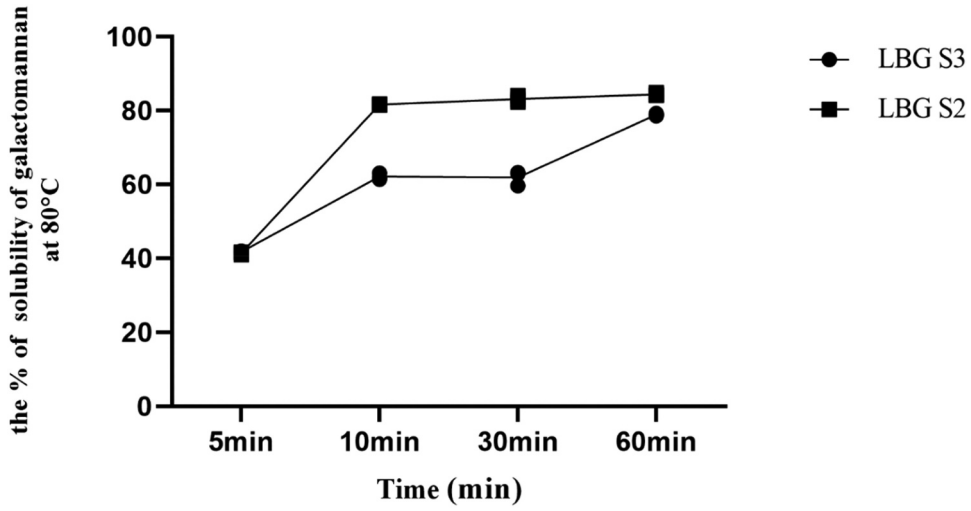

Figure 3. The solubility kinetics at 80°C of galactomannan (LBG) from the endosperm of the unripe stage (LBG.S2) and ripe stage (LBG.S3) carob seeds.

S2 and 65.82 ± 0.65% for LBG.S3. At 80°C, the solubility of galactomannan was rapid, but a significant difference ($p < 0.05$) persisted between LBG.S2 and LBG.S3. After 10 minutes, LBG.S2 exhibited a solubility rate of 81.63 ± 0.16%, while LBG.S3 had a rate of 62.09 ± 0.83%. Remarkably, the solubility rates at 10 minutes were comparable to those achieved in three hours at 25°C. The maximum solubility rates after one hour were 84.39 ± 0.39% for LBG.S2 and 78.87 ± 0.34% for LBG.S3.

Locust bean gum exhibits partial solubility in cold water and requires heating to achieve its maximum solubility.[17] The variation in solubility between LBG.S2 and LBG.S3 is attributed, as previously mentioned, to the M/G ratio, which is a key factor influencing the solubility of galactomannan polysaccharides. Higher galactose substitution leads to increased solubility due to the relatively hydrophobic nature of the mannose chains and the more hydrophilic nature of the galactose units.[53] The M/G ratio in unripe seeds is lower than that of the ripe seeds due to the removal of galactosyl groups from mannose chains by α-galactosidase in the endosperm.[50] Our findings align with the research of Dakia, Blecker,[10] who observed that LBG exhibits partial solubility in cold water (50% at 25°C/1 h) and requires heating to achieve its maximum solubility (70–85% at 80°C/30 min). Furthermore, Sébastien, Christophe[54] investigated the influence of extraction temperature on LBG solubility. They observed a direct correlation between the extraction temperature of galactomannan and the temperature needed for its dissolution in water. This was achieved using a water bath method at temperatures of 25°C and 80°C. Various factors contribute to the solubility of galactomannan powder, including the source of galactomannan, the solvent used, the method of drying, the conditions of processing, the immersion suitability, and the solute's structure.[36]

Emulsion properties

The incorporation of polysaccharide as a stabilizer in "oil-in-water" emulsions enhances the textural properties and increases the viscosity of the aqueous phase.[55] Based on the results obtained regarding the emulsifying properties of LBG.S2 and LBG.S3 at a concentration of 1% (w/v) (Table 6), both samples exhibited remarkably high emulsifying capacity, with values of 71.15 ± 3.33% for LBG.S2 and 76.28 ± 1.10% for LBG.S3, indicating strong emulsifying properties. A significant difference between the two samples was observed ($p = 0.031$). However, upon subjecting the emulsions of both LBG to heat treatment at 80°C

Table 6. Functional properties of galactomannan from ripe (LBG.S3) and unripe (LBG.S2) carob seeds (endosperm).

Functional properties Of galactomannan	Yield (%)	Emulsion capacity (%)	Emulsion stability (%)	Water holding capacity (WHC) (g water/g sample)	Oil holding capacity (OHC) (g oil/g sample)	Viscosity η (mPa·s)
LBG.S2	56.73 ± 2.76	71.15 ± 3.33	66.44 ± 0.38	9.43 ± .90	6.73 ± .15	4.00 ± .02
LBG.S3	47.53 ± 2.55	76.28 ± 1.10	66.79 ± 0.05	23.4 ± .2	9.8 ± .4	4.94 ± .01

LBG.S2: galactomannan extracted from carob seeds harvested in the semi-ripe stage.
LBG.S3: galactomannan extracted from carob seeds harvested in the ripe stage.

for 30 minutes, the stability decreased to 66.44 ± 0.38% for both samples, and a significant decrease was noted ($p < 0.05$) in both cases, particularly for LBG.S3.

Our results outperform the emulsion capacity and emulsion stability of LBG extracted by using water bath at 80°C (for 1 h) reported by Wu et al.,[56] which were approximately 44% and 41%, respectively. This difference can be attributed to variations in the extraction and purification methods, as well as the origin and harvesting period of carob seeds. The disparity between the two LBG samples is linked to the M/G ratio, as molecules with higher M/G ratios can form intermolecular associations between non-substituted regions in the mannan skeleton, while samples with lower M/G ratios can form a more gel-like layer around the oil droplets, thus improving the emulsion capacity and stability.[57]

Polysaccharides play a significant role in emulsions by providing water retention and thickening properties.[58] Once a successful emulsion is formed, its long-term stability relies on the polymer's ability to create a barrier at the interface, preventing droplets from aggregating or merging[59] However, after subjecting the emulsions to higher temperature (80°C, 30 min), this barrier around the oil droplets is disrupted, leading to emulsion destabilization.[56]

Water holding capacity (WHC) and oil holding capacity (OHC)

The water holding capacity (WHC) of galactomannan refers to the ability of the substance to retain moisture under specific conditions, and it is essential for determining storage parameters and evaluating its suitability for use in food preparations.[60] The findings derived from the effect analysis of LBG.S2 and LBG.S3 on the water and oil holding capacity (WHC, OHC) (Table 6) indicated a significant difference ($p < 0.0001$) between the two stages of ripening for both WHC and OHC. Additionally, there were differences in WHC and OHC values within the same ripening stage.

The water holding capacity of LBG.S3 (23.4 ± 0.2 g of water/g of sample) was found to be significantly higher ($p < 0.0001$) than that of LBG.S2 (9.43 ± 0.90 g of water/g of sample). These values are superior to those the reported by Niknam et al.[36] for the WHC of galactomannan extracted from Fenugreek Seeds (215.05 ± 0.879 g of water/100 g of galactomannan) and the WHC of guar galactomannan (241.2 g of water/100 g of galactomannan).[61] Galactomannan's water holding capacity (WHC) is affected by a number of variables, including the presence of hydroxyl groups, the extraction process, the porosity of the material, and the amount of protein in its structure.[36]

On the other hand, the oil holding capacity (OHC) is an important characteristic of galactomannans, which refers to their ability to retain oil.[36] The OHC of LBG.S3 was measured at 9.8 ± 0.4 g of oil per gram of sample, which was significantly higher ($p < 0.0001$) than that of LBG.S2 (6.73 ± 0.15 g of oil per gram of sample). These values were significantly higher than those that were reported by Niknam et al.[36] for other galactomannans, such as 60.2 ± 0.08 g of oil per 100 g of galactomannan, and the values reported by Rashid, Hussain and Ahmed[61] for guar galactomannan (41.52 g of oil/100 g of galactomannan). As reported by Thanatcha and Pranee,[62] the ability of hydrocolloids to hold oil typically count on the existence of nonpolar groups that can interact with and hold onto oil molecules. According to by Niknam et al.,[36] The OHC value is also influenced by the structural and chemical characteristics of galactomannans, particularly the distribution of hydrophobic to hydrophilic groups within their structure.

Viscosity

The viscosity results of the two samples extracted using optimal condition of UAE at a concentration of 0.1% (Table 6) reveal that the LBG.S3 solution exhibits significantly higher viscosity ($p < 0.0001$) compared to the LBG.S2 solution. These findings are consistent with the research conducted by Liu et al.,[50] which indicates that the apparent viscosity of galactomannan extracted at 70°C for 3 h in water bath and kept on a water bath with mechanical stirring varies depending on the developmental stages of *Gleditsia sinensis* Lam. The viscosity of galactomannan extracted from carob endosperm is influenced by several factors, including molecular weight, solubilization method, shear rate, and concentration. Generally, the viscosity increases as the gum concentration rises.[17] The viscosity observed in galactomannan dispersions arises from two primary factors. Firstly, it is a result of the interpenetration of macromolecular chains, leading to nonspecific "physical" recovery. Secondly, it is due to the existence of highly specialized interactions between macromolecules, resulting from intermolecular aggregation phenomena (hyper-entanglements) as indicated by Sébastien et al..[54]

Fourier-transform infrared spectroscopy (FT-IR) analysis

FT-IR spectroscopy is commonly employed to identify the functional groups present in different materials, including galactomannans. Figure 4 reveal the FT-IR

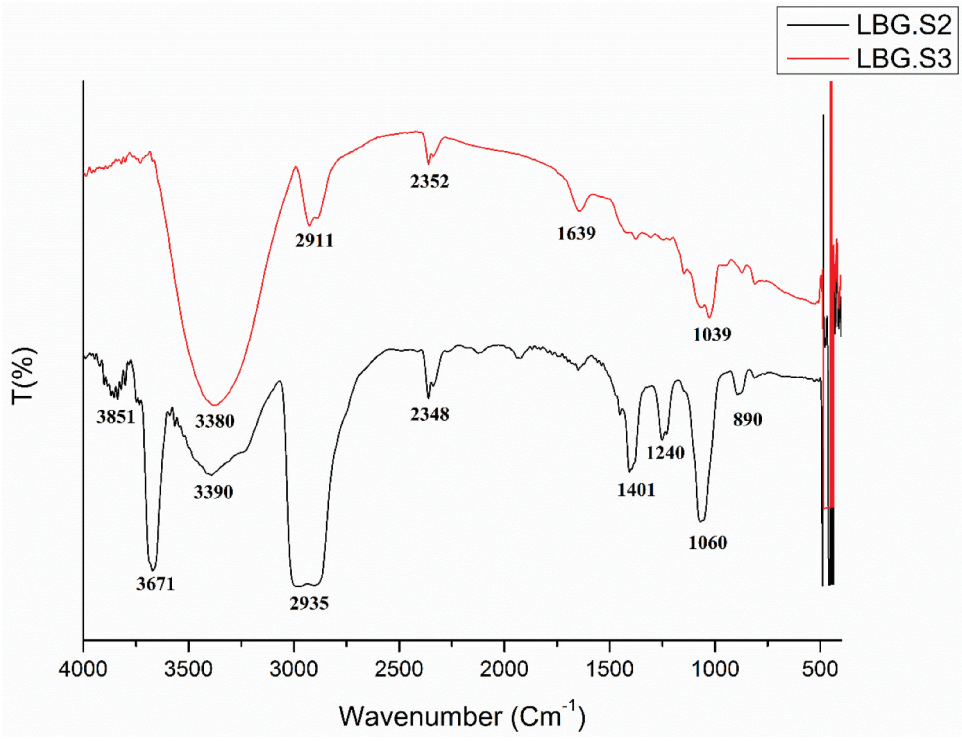

Figure 4. FT-IR spectrum of galactomannan extracted from the endosperm of ripe (LBG.S3) and unripe (LBG.S2) carob seeds.

spectra of galactomannan extracted from both ripe and unripe carob seeds. according to the analysis of the infrared spectra of galactomannan we notice that the LBG.S2 is characterized by special absorption bands which are not found in the spectrum of LBG.S3 such as the absorption band at 3851 cm^{-1} which has been allotted to possible functional groups of Ge-ZnO NPs.[63] The absorption band at 3671 cm^{-1} showed axial distortion of O – H, matching to intermolecular hydrogen bonding and intramolecular.[64] The broad band at 3390 cm^{-1} was characteristic of the hydroxyl group.[65] The absorption band at 2935 cm^{-1} was attributed to the stretching vibration (C-H) of the C-H bond.[66] The absorption band at 2348 cm^{-1} is more related to the CH_2 stretching and swinging vibrations of the polysaccharides.[67] The 1401 cm^{-1} band is the bending vibration of COH groups and the antisymmetric stretching band of C – O – C groups of polysaccharides.[68] The absorption band at 1240 cm^{-1} corresponds to S=O of sulfate esters.[69] The enhancement of the peaks at 1650 cm^{-1} may be owing to the combination of amides and carbonyl groups with other substituents.[70] The band at 890 cm^{-1} was attributed to Bending C1–H.[71]

Several peaks have disappeared with the galactomannan (LBG.S3) extracted from the ripe carob seeds, LBG. S3 indicates an O-H stretching absorption peak at wavelength 3380 cm^{-1}.[72] The absorption band at 2911 cm^{-1} is due to C – H stretching.[73] Peak absorption 2352 cm^{-1} indicated P – O bending.[74] The absorption bands at 1639 cm^{-1} were assigned to the stretching vibration of the C – O bond of the carboxyl group.[75] The absorption bands at 1039 were attributed to a C – C (galactan) stretching ring.[71] LBG.S2 and LBG.S3 possess distinct chemical compositions, attributed to the presence of functional groups in LBG.S2 that are absent in LBG.S3. Our findings corroborate the prior study conducted by Liu et al.,[50] demonstrating that the Mannose/Galactose (M/G) ratio of galactomannan in *Gleditsia sinensis* Lam fruits undergoes an initial increase followed by a decrease during fruit ripening. This implies that in the early stages of biosynthesis, the galactomannan backbone is fully substituted, and subsequently, some galactosyl groups are enzymatically removed by α-galactosidase in the endosperm.

Anti-inflammatory activity

Inhibition of bovine serum albumin (BSA) protein denaturation

Protein denaturation is widely recognized as a contributing factor to inflammatory and arthritic diseases.[76] Inflammatory processes are often linked to pain and encompass various conditions, including protein denaturation and membrane impairment.[77] In the present work, the anti-inflammatory properties

of galactomannan extracted from carob seeds (LBG.S2 and LBG.S3) were assessed using a bovine serum albumin test. The effect of galactomannan on the denaturation of the BSA is dose-dependent relationship. In fact, the activity was increased with increasing concentration of LBG.S2, and LBG.S3 (Figure 5). The LBG.S3 has been shown to provide protection of 12.32 ± 2.07% to 43.73 ± 0.46% against BSA heat denaturation at concentrations ranging from 50 µg/mL to 1000 µg/mL respectively. In addition, the LBG.S2 was found to provide protection of 9.93 ± 0.75% to 46.68 ± 0.86% against BSA denaturation at the same concentrations, respectively. According to the statistical analysis, which shows that there is a highly significant difference ($p < 0.0001$) between most of the different concentrations of LBG.S2 and LBG.S3, which shows protection against thermal denaturation of BSA.

Our findings are in accordance with the research conducted by Ibanoglu[78] regarding the thermal denaturation of BSA in the presence of hydrocolloids like pectin, guar gum, and i-carrageenan. It was noted that the increase in the enthalpy of BSA denaturation, when hydrocolloids were present, could be attributed to the protective effect on globular proteins. This protection is achieved by obstructing the hydrophobic binding sites of proteins through the bulky polysaccharide component. According to Yang and Zhang,[79] polysaccharides derived from natural sources exhibit a variety of biological activities that are influenced by their chemical structures and chain conformations.

Membrane stabilization test

The utilization of erythrocyte membranes is highly significant for in vitro studies of anti-inflammatory activity, as it helps to restrict the inflammatory response by preventing the release of lysosomal constituents from activated neutrophils. Additionally, the erythrocyte membrane serves as an analogue to the lysosomal membrane.[80]

The results of erythrocyte membrane stabilization present in Figure 6 show that LBG exhibits a very strong inhibition of hemolysis of red blood cells, which is dose-dependent, in fact, the activity was increased with increasing concentration of LBG.S2 and LBG.S3. Where the LBG.S3 has a very strong inhibition of hemolysis of red blood cells at different concentrations ranging from 50 to 1000 µg/ml where the percentage of inhibition was from 13.33 ± 2.65% to 86.23 ± 1.34% respectively. While LBG.S2 has inhibition of 9.15 ± 1.62 to 78.36 ± 3.51% at the same concentrations, respectively. The statistical analysis reveals a highly significant difference ($p < 0.0001$) between the results of nearly all the studied concentrations for both samples (LBG.S3 and LBG.S2), likely attributed to the biosynthesis of galactomannan during maturation, as indicated by Liu et al..[50] When red blood cells are exposed to a hypotonic solution, their permeability increases, allowing fluids to enter and accumulate inside the cell, ultimately leading to the rupture of its membrane. The damage to the membrane of red blood cells renders them more susceptible to secondary harm caused by lipid peroxidation initiated by free radicals.[81]

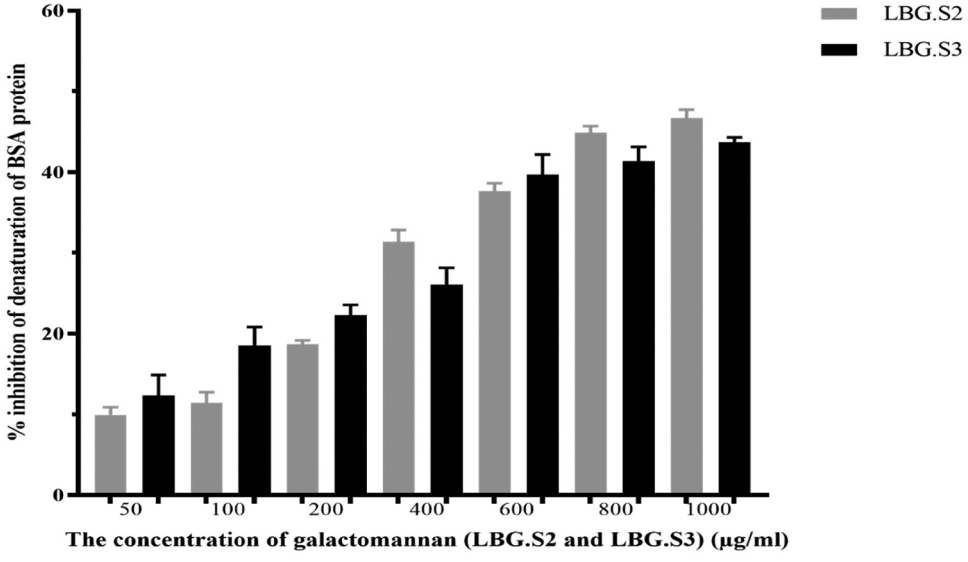

Figure 5. The percentage of inhibition of denaturation of protein BSA by galactomannan (LBG) extracted from the semi-ripe stage (LBG.S2) and ripe stage (LBG.S3) carob seeds.

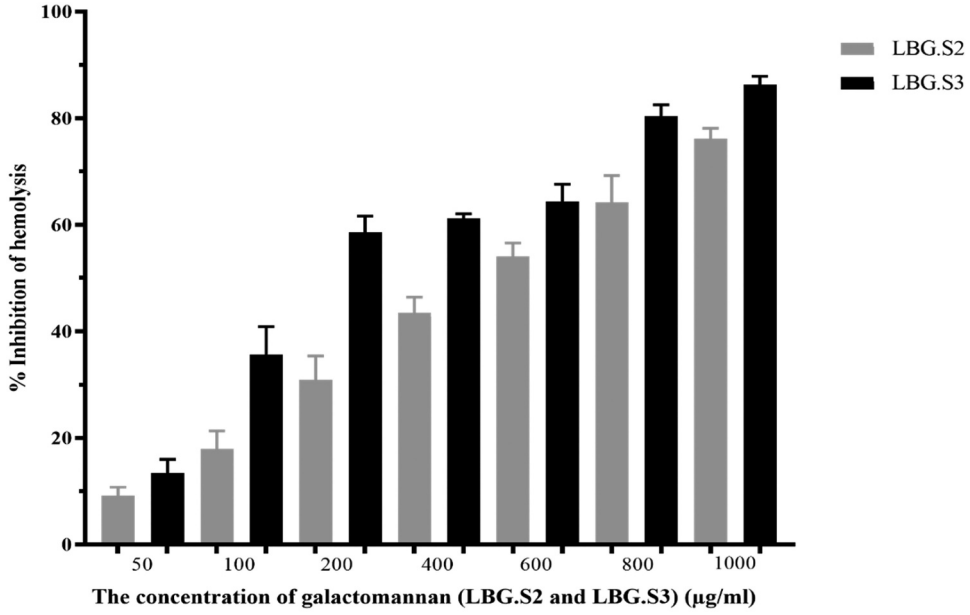

Figure 6. The percentage of inhibition of hemolysis of galactomannan from the endosperm of the unripe stage (LBG.S2) and ripe stage (LBG.S3) carob seeds.

The precise mechanism by which membranes are stabilized is still unknown, it's possible that the extract accomplishes this effect by changing the surface-to-volume ratio of cells via mechanisms such as membrane stretching, cell contraction, and interactions with membrane proteins.[39] Previous studies[39,82] have also indicated that when erythrocytes are exposed to a hypotonic environment, their membrane may experience rupture due to cell contraction, leading to osmotic loss of electrolytes. The membrane stabilization process caused by the hypotonic solution involves preventing the migration of these components from inside the cell to the outside. Additionally, it has been observed that cellular deformation and erythrocyte size are closely related to their intracellular calcium content, as well as the stabilization of skeletal proteins.[83] Therefore, the polysaccharides extracted from carob seeds may exhibit similar effects to nonsteroidal anti-inflammatory drugs, which are known to exert their beneficial effects through mechanisms such as stabilizing lysosomal membranes or inhibiting the release of lysosomal enzymes.[84]

Conclusion

The characteristics of extracted polysaccharides are greatly influenced by various extraction, purification, and drying processes. A high yield of galactomannan (47.53 ± 2.55%) was extracted under the optimal extraction conditions. As a result, the obtained galactomannan's physicochemical and functional properties were significantly affected by the use of ultrasound, proving that the extraction and purification processes were successfully carried out. LBG.S2 exhibited a higher yield compared to LBG.S3. The FT-IR analysis revealed the existence of certain functional groups in unripe seeds, which disappeared in LBG.S3, suggesting changes in galactomannan biosynthesis during maturation. Both polysaccharides demonstrated important functional properties, particularly the galactomannan extracted from ripe carob seeds. Moreover, galactomannan exhibited anti-inflammatory activity, as evidenced by its anti-hemolytic and heat-induced protein denaturation inhibition effects. These findings provide valuable insights into the potential future applications of galactomannan extracted from carob seeds as a natural polysaccharide in the realms of the food, pharmaceutical, and cosmetic sectors.

Disclosure statement

No potential conflict of interest was reported by the author(s).

References

[1] Batlle, I., Tous, J. *Carob Tree: Ceratonia Siliqua L.- Promoting the Conservation and Use of Underutilized and Neglected Crops. 17* ; Rome, Italy: Bioversity International, 1997; Vol. 17.

[2] Othmen, K. B., Elfalleh, W., García Beltrán, J M., Esteban, M Á., Haddad, M. An in vitro study of the effect of carob (Ceratonia siliqua L.) leaf extracts on gilthead seabream (Sparus aurata L.) leucocyte

activities. Antioxidant, cytotoxic and bactericidal properties. *Fish & Shellfish Immunology*. 2020, *99*, 35–43. DOI: 10.1016/j.fsi.2020.02.005.

[3] Farag, M. A.; El-Kersh, D. M.; Ehrlich, A.; Choucry, M. A.; El-Seedi, H.; Frolov, A.; Wessjohann, L. A. Variation in Ceratonia siliqua pod metabolome in context of its different geographical origin, ripening stage and roasting process. *Food Chem*. 2019, *283*, 675–687. DOI: 10.1016/j.foodchem.2018.12.118.

[4] Battle, I.; Tous, J. *Carob Tree: Ceratonia Siliqua L.-Promoting the Conservation and Use of Underutilized and Neglected Crops. 17*; Rome.Italy: Bioversity International, 1997.

[5] Hostettler, M.; Steffen, R.; Tschopp, A. Efficacy and Tolerance of Insoluble Carob Fraction in the Treatment of Travellers. *Diarrhoea. J. Diarrhoeal Diseases Res*. 1995, 13, 155–158.

[6] Gulay, M.; Yildiz-Gul, O.; Ata, A.; Balic, A.; Demirtas, A. Toxicological evaluation of carob (Ceratonia silique) bean extracts in male New Zealand White rabbits. *J. Anim. Vet. Adv*. 2012, *11*(11), 1853–1857. DOI: 10.3923/javaa.2012.1853.1857.

[7] Durazzo, A.; Turfani, V.; Narducci, V.; Azzini, E.; Maiani, G.; Carcea, M. Nutritional Characterisation and Bioactive Components of Commercial Carobs Flours. *Food Chem*. 2014, *153*, 109–113. DOI: 10.1016/j.foodchem.2013.12.045.

[8] Papagiannopoulos, M.; Wollseifen, H. R.; Mellenthin, A.; Haber, B.; Galensa, R. Identification and quantification of polyphenols in Carob Fruits (Ceratonia siliqua L.) and derived products by HPLC-UV-ESI/MS n. *J. Agric. Food Chem*. 2004, *52* (12), 3784–3791. DOI: 10.1021/jf030660y.

[9] Loullis, A.; Pinakoulaki, E. Carob as Cocoa Substitute: A Review on Composition, Health Benefits and Food Applications. *Eur. Food Res. Technol*. 2018, *244*(6), 959–977. DOI: 10.1007/s00217-017-3018-8.

[10] Dakia, P. A.; Blecker, C.; Robert, C.; Wathelet, B.; Paquot, M. Composition and Physicochemical Properties of Locust Bean Gum Extracted from Whole Seeds by Acid or Water Dehulling Pre-Treatment. *Food Hydrocolloids*. 2008, *22*(5), 807–818. DOI: 10.1016/j.foodhyd.2007.03.007.

[11] Santonocito, D.; Granata, G.; Geraci, C.; Panico, A.; Siciliano, E. A.; Raciti, G.; Puglia, C. Carob Seeds: Food Waste or Source of Bioactive Compounds? *Pharmaceutics*. 2020, *12*(11), 1090. DOI: 10.3390/pharmaceutics12111090.

[12] Lazaridou, A.; Biliaderis, C. G.; Izydorczyk, M. S. Structural Characteristics and Rheological Properties of Locust Bean Galactomannans: A Comparison of Samples from Different Carob Tree Populations. *J. Sci. Food Agric*. 2001, *81*(1), 68–75. DOI: 10.1002/1097-0010(20010101)81:1<68:AID-JSFA780>3.0.CO;2-G.

[13] Bouzouita, N.; KHALDI, A.; ZGOULLI, S.; CHEBIL, L.; CHEKKI, R.; CHAABOUNI, M.; THONART, P. The Analysis of Crude and Purified Locust Bean Gum: A Comparison of Samples from Different Carob Tree Populations in Tunisia. *Food Chem*. 2007, *101*(4), 1508–1515. DOI: 10.1016/j.foodchem.2006.03.056.

[14] Fidan, H.; Stankov, S.; Petkova, N.; Petkova, Z.; Iliev, A.; Stoyanova, M.; Ivanova, T.; Zhelyazkov, N.; Ibrahim, S.; Stoyanova, A., et al. Evaluation of Chemical Composition, Antioxidant Potential and Functional Properties of Carob (Ceratonia Siliqua L.) Seeds. *J. Food Sci. Technol*. 2020, *57*(7), 2404–2413.

[15] Dakia, P. A.; Wathelet, B.; Paquot, M. *Influence de la teneur en galactose sur les interactions moléculaires et sur les propriétés physico-chimiques des galactomannanes en solution*; Belgique: BASE, 2010.

[16] Biner, B.; Gubbuk, H.; Karhan, M.; Aksu, M.; Pekmezci, M. Sugar Profiles of the Pods of Cultivated and Wild Types of Carob Bean (Ceratonia Siliqua L.) in Turkey. *Food Chem*. 2007, *100*(4), 1453–1455. DOI: 10.1016/j.foodchem.2005.11.037.

[17] Barak, S.; Mudgil, D. Locust Bean Gum: Processing, Properties and Food Applications—A Review. *Int. J. Biol. Macromol*. 2014, *66*, 74–80. DOI: 10.1016/j.ijbiomac.2014.02.017.

[18] Bosch, J.; Del Pino, F. G.; Ramoneda, J.; Retana, J. *Fruiting Phenology and Fruit Set of Carob, Ceratonia Siliqua L. (Cesalpinaceae)*. Israel. *J. Plant Sci*. 1996, *44* (4), 359–368. DOI: 10.1080/07929978.1996.10676657.

[19] Benchikh, Y.; Louaileche, H.; George, B.; Merlin, A. Changes in Bioactive Phytochemical Content and in vitro Antioxidant Activity of Carob (Ceratonia Siliqua L.) as Influenced by Fruit Ripening. *Ind. Crops Prod*. 2014, *60*, 298–303. DOI: 10.1016/j.indcrop.2014.05.048.

[20] Saci, F.; Bachir Bey, M.; Louaileche, H.; Gali, L.; Bensouici, C. Changes in Anticholinesterase, Antioxidant Activities and Related Bioactive Compounds of Carob Pulp (Ceratonia Siliqua L.) During Ripening Stages. *J. Food Meas. Charact*. 2020, *14*(2), 937–945. DOI: 10.1007/s11694-019-00344-9.

[21] Jiang, J.; Kong, F.; Li, N.; Zhang, D.; Yan, C.; Lv, H. *Purification, Structural Characterization and in vitro Antioxidant Activity of a Novel Polysaccharide from Boshuzhi*. Carbohydrate Polymers. *Carbohydr. Polym*. 2016, *147*, 365–371. DOI: 10.1016/j.carbpol.2016.04.001.

[22] Li, Q.; Feng, Y.; He, W.; Wang, L.; Wang, R.; Dong, L.; Wang, C. Post-Screening Characterisation and in vivo Evaluation of an Anti-Inflammatory Polysaccharide Fraction from Eucommia Ulmoides. *Carbohydr. Polym*. 2017, *169*, 304–314. DOI: 10.1016/j.carbpol.2017.04.034.

[23] Mzoughi, Z.; Abdelhamid, A.; Rihouey, C.; Le Cerf, D.; Bouraoui, A.; Majdoub, H. Optimized extraction of pectin-like polysaccharide from Suaeda fruticosa leaves: Characterization, antioxidant, anti-inflammatory and analgesic activities. *Carbohydr. Polym*. 2018, *185*, 127–137. DOI: 10.1016/j.carbpol.2018.01.022.

[24] Qi, J.; Kim, S. M. Characterization and immunomodulatory activities of polysaccharides extracted from green alga Chlorella ellipsoidea. *Int. J. Biol. Macromol*. 2017, *95*, 106–114. DOI: 10.1016/j.ijbiomac.2016.11.039.

[25] Chen, H.; Sun, J.; Liu, J.; Gou, Y.; Zhang, X.; Wu, X.; Sun, R.; Tang, S.; Kan, J.; Qian, C., et al. Structural Characterization and Anti-Inflammatory Activity of Alkali-Soluble Polysaccharides from Purple Sweet Potato. *Int. J. Biol. Macromol*. 2019, *131*, 484–494. DOI: 10.1016/j.ijbiomac.2019.03.126.

[26] Jeddou, K. B.; Chaari, F.; Maktouf, S.; Nouri-Ellouz, O.; Helbert, C. B.; Ghorbel, R. E. Structural, Functional, and

Antioxidant Properties of Water-Soluble Polysaccharides from Potatoes Peels. *Food Chem*. 2016, *205*, 97–105. DOI: 10.1016/j.foodchem.2016.02.108.

[27] Alamgir, A. *Therapeutic Use of Medicinal Plants and Their Extracts: Volume 1*; Berlin (Allemagne): Springer, 2017.

[28] Vilkhu, K., Mawson, R., Simons, L., Bates, D. Applications and Opportunities for Ultrasound Assisted Extraction in the Food Industry—A Review. *Innovative Food Science & Emerging Technologies*. 2008, *9*(2), 161–169. 10.1016/j.ifset.2007.04.014

[29] Tiwari, B. K. *Ultrasound: A Clean, Green Extraction Technology*. TrAc Trends in Analytical Chemistry. *TrAc Trends Anal. Chem*. 2015, *71*, 100–109. DOI: 10.1016/j.trac.2015.04.013.

[30] Gallo, M.; Ferrara, L.; Naviglio, D. Application of Ultrasound in Food Science and Technology: A Perspective. *Foods*. 2018, *7*(10), 164. DOI: 10.3390/foods7100164.

[31] Rodrigues, S.; Fernandes, F. A. *Extraction Processes Assisted by ultrasound*, in *Ultrasound: Advances for Food Processing and Preservation*. *Elsevier*. 2017, 1, 351–368.

[32] Fernandes, F. A. N.; Gallão, M. I.; Rodrigues, S. Effect of Osmosis and Ultrasound on Pineapple Cell Tissue Structure During Dehydration. *J. Food Eng*. 2009, *90* (2), 186–190. DOI: 10.1016/j.jfoodeng.2008.06.021.

[33] Rodrigues, S.; Gomes, M. C.; Gallão, M. I.; Fernandes, F. A. Effect of Ultrasound-Assisted Osmotic Dehydration on Cell Structure of Sapotas. *J. Sci. Food Agric*. 2009, *89*(4), 665–670. DOI: 10.1002/jsfa.3498.

[34] Amid, B. T.; Mirhosseini, H. Optimisation of Aqueous Extraction of Gum from Durian (Durio Zibethinus) Seed: A Potential, Low Cost Source of Hydrocolloid. *Food Chem*. 2012, *132*(3), 1258–1268. DOI: 10.1016/j.foodchem.2011.11.099.

[35] Wang, L.; Zhang, B.; Xiao, J.; Huang, Q.; Li, C.; Fu, X. Physicochemical, Functional, and Biological Properties of Water-Soluble Polysaccharides from Rosa Roxburghii Tratt Fruit. *Food Chem*. 2018, *249*, 127–135. DOI: 10.1016/j.foodchem.2018.01.011.

[36] Niknam, R.; Mousavi, M.; Kiani, H. New Studies on the Galactomannan Extracted from Trigonella Foenum-Graecum (Fenugreek) Seed: Effect of Subsequent Use of Ultrasound and Microwave on the Physicochemical and Rheological Properties. *Food Bioprocess. Technol*. 2020, *13*(5), 882–900. DOI: 10.1007/s11947-020-02437-6.

[37] Bostanudin, M. F.; Arafat, M.; Sarfraz, M.; Górecki, D. C.; Barbu, E. Butylglyceryl Pectin Nanoparticles: Synthesis, Formulation and Characterization. *Polymers*. 2019, *11*(5), 789. DOI: 10.3390/polym11050789.

[38] Lekouaghet, A.; Boutefnouchet, A.; Bensuici, C.; Gali, L.; Ghenaiet, K.; Tichati, L. In vitro Evaluation of Antioxidant and Anti-Inflammatory Activities of the Hydroalcoholic Extract and Its Fractions from Leuzea Conifera L. Roots. *South African J. Of Bot*. 2020, *132*, 103–107. DOI: 10.1016/j.sajb.2020.03.042.

[39] Shinde, U.; Phadke, A. S.; Nair, A. M.; Mungantiwar, A. A.; Dikshit, V. J.; Saraf, M. N. Membrane Stabilizing Activity—A Possible Mechanism of Action for the Anti-Inflammatory Activity of Cedrus Deodara Wood Oil. *Fitoterapia*. 1999, *70*(3), 251–257. DOI: 10.1016/S0367-326X(99)00030-1.

[40] Zhongdong, L.; Guohua, W.; Yunchang, G.; Kennedy, J. F. Image Study of Pectin Extraction from Orange Skin Assisted by Microwave. *Carbohydr. Polym*. 2006, *64*(4), 548–552. DOI: 10.1016/j.carbpol.2005.11.006.

[41] XuJie, H.; Wei, C. Optimization of Extraction Process of Crude Polysaccharides from Wild Edible BaChu Mushroom by Response Surface Methodology. *Carbohydr. Polym*. 2008, *72*(1), 67–74. DOI: 10.1016/j.carbpol.2007.07.034.

[42] Ye, C.-L.; Jiang, C.-J. Optimization of Extraction Process of Crude Polysaccharides from Plantago Asiatica L. by Response Surface Methodology. *Carbohydr. Polym*. 2011, *84*(1), 495–502. DOI: 10.1016/j.carbpol.2010.12.014.

[43] Ying, Z.; Han, X.; Li, J. Ultrasound-Assisted Extraction of Polysaccharides from Mulberry Leaves. *Food Chem*. 2011, *127*(3), 1273–1279. DOI: 10.1016/j.foodchem.2011.01.083.

[44] Zhao, S.; Kwok, K.-C.; Liang, H. Investigation on Ultrasound Assisted Extraction of Saikosaponins from Radix Bupleuri. *Sep. Purif. Techn*. 2007, *55*(3), 307–312. DOI: 10.1016/j.seppur.2006.12.002.

[45] Maran, J. P.; Manikandan, S.; Thirugnanasambandham, K.; Vigna Nivetha, C.; Dinesh, R. Box–Behnken design based statistical modeling for ultrasound-assisted extraction of corn silk polysaccharide. *Carbohydr. Polym*. 2013, *92*(1), 604–611. DOI: 10.1016/j.carbpol.2012.09.020.

[46] RenJie, L. Optimization of Extraction Process of Glycyrrhiza Glabra Polysaccharides by Response Surface Methodology. *Carbohydr. Polym*. 2008, *74*(4), 858–861. DOI: 10.1016/j.carbpol.2008.05.005.

[47] Yin, G.; Dang, Y. Optimization of Extraction Technology of the Lycium Barbarum Polysaccharides by Box–Behnken Statistical Design. *Carbohydr. Polym*. 2008, *74*(3), 603–610. DOI: 10.1016/j.carbpol.2008.04.025.

[48] Sun, Y.; Liu, J.; Kennedy, J. F. Application of Response Surface Methodology for Optimization of Polysaccharides Production Parameters from the Roots of Codonopsis Pilosula by a Central Composite Design. *Carbohydr. Polym*. 2010, *80*(3), 949–953. DOI: 10.1016/j.carbpol.2010.01.011.

[49] Abe, E.; Delyle, S. G.; Alvarez, J. C. Extraction liquide-liquide: théorie, applications, difficultés. In *Annales de Toxicologie Analytique*; Société Française de Toxicologie Analytique, Ed.; France: EDP Sciences, 2010; pp. 51–59.

[50] Liu, Y.; Xu, W.; Lei, F.; Li, P.; Jiang, J. Comparison and Characterization of Galactomannan at Different Developmental Stages of Gleditsia Sinensis Lam. *Carbohydr. Polym*. 2019, *223*, 115127. DOI: 10.1016/j.carbpol.2019.115127.

[51] Bhattacharyya, S. B.; Das, A. K.; Banerji, N.; Farooqi, M. I. H. A Water-Soluble Galactomannan from Sesbania Aegyptiaca Seeds. *Phytochemistry*. 1983, *22*(1), 161–164. DOI: 10.1016/S0031-9422(00)80078-3.

[52] Trabelsi, I.; Slima, S. B.; Ktari, N.; Bardaa, S.; Elkaroui, K.; Abdeslam, A.; Ben Salah, R. Purification, Composition and Biological Activities of a Novel Heteropolysaccharide Extracted from Linum Usitatissimum L. Seeds on Laser Burn Wound. *Int. J. Biol. Macromol.* 2020, *144*, 781–790. DOI: 10.1016/j.ijbiomac.2019.10.077.

[53] Dionísio, M.; Grenha, A. Locust bean gum: exploring its potential for biopharmaceutical applications. *J. Pharm. Bioall. Sci.* 2012, *4*(3), 175. DOI: 10.4103/0975-7406.99013.

[54] Sébastien, G.; Christophe, B.; Mario, A.; Pascal, L.; Michel, P.; Aurore, R. Impact of Purification and Fractionation Process on the Chemical Structure and Physical Properties of Locust Bean Gum. *Carbohydr. Polym.* 2014, *108*, 159–168. DOI: 10.1016/j.carbpol.2014.02.092.

[55] Farshchi, A.; Ettelaie, R.; Holmes, M. Influence of pH Value and Locust Bean Gum Concentration on the Stability of Sodium Caseinate-Stabilized Emulsions. *Food Hydrocolloids*. 2013, *32*(2), 402–411. DOI: 10.1016/j.foodhyd.2013.01.010.

[56] Wu, Y.; Cui, W.; Eskin, N. A. M.; Goff, H. D. An Investigation of Four Commercial Galactomannans on Their Emulsion and Rheological Properties. *Food Res. Int.* 2009, *42*(8), 1141–1146. DOI: 10.1016/j.foodres.2009.05.015.

[57] Dea, I. C.; Clark, A. H.; McCleary, B. V. Effect of Galactose-Substitution-Patterns on the Interaction Properties of Galactomannas. *Carbohydr. Res.* 1986, *147*(2), 275–294. DOI: 10.1016/S0008-6215(00)90637-2.

[58] Dickinson, E. Hydrocolloids at Interfaces and the Influence on the Properties of Dispersed Systems. *Food Hydrocolloids*. 2003, *17*(1), 25–39. DOI: 10.1016/S0268-005X(01)00120-5.

[59] Dickinson, E.; Euston, S. R. Computer Simulation Model of the Adsorption of Protein—Polysaccharide Complexes. *Food Hydrocolloids*. 1992, *6*(4), 345–357. DOI: 10.1016/S0268-005X(09)80002-7.

[60] Chang, Y.; Cui, S. W.; Roberts, K. T.; Ng, P. K. W.; Wang, Q. Evaluation of extrusion-modified fenugreek gum. *Food Hydrocolloids*. 2011, *25*(5), 1296–1301. DOI: 10.1016/j.foodhyd.2010.12.003.

[61] Rashid, F.; Hussain, S.; Ahmed, Z. Extraction Purification and Characterization of Galactomannan from Fenugreek for Industrial Utilization. *Carbohydr. Polym.* 2018, *180*, 88–95. DOI: 10.1016/j.carbpol.2017.10.025.

[62] Thanatcha, R.; Pranee, A. Extraction and Characterization of Mucilage in Ziziphus Mauritiana Lam. *Int. Food Res. J.* 2011, *18*(1), 55–58. DOI: 10.54207/bsmps2000-2011-IS47HQ.

[63] Divya, M.; Vaseeharan, B.; Abinaya, M.; Vijayakumar, S.; Govindarajan, M.; Alharbi, N. S.; Kadaikunnan, S.; Khaled, J. M.; Benelli, G. Biopolymer Gelatin-Coated Zinc Oxide Nanoparticles Showed High Antibacterial, Antibiofilm and Anti-Angiogenic Activity. *J. Photochem. Photobiol. B Biol.* 2018, *178*, 211–218. DOI: 10.1016/j.jphotobiol.2017.11.008.

[64] Paiva, A. A. D. O.; Castro, A. J. G.; Nascimento, M. S.; Will, L. S. E. P.; Santos, N. D.; Araújo, R. M.; Xavier, C. A. C.; Rocha, F. A.; Leite, E. L. Antioxidant and Anti-Inflammatory Effect of Polysaccharides from Lobophora Variegata on Zymosan-Induced Arthritis in Rats. *Int. Immunopharmacol.* 2011, *11*(9), 1241–1250. DOI: 10.1016/j.intimp.2011.04.003.

[65] Pan, D.; Wang, L.; Chen, C.; Teng, B.; Wang, C.; Xu, Z.; Hu, B.; Zhou, P. Structure Characterization of a Novel Neutral Polysaccharide Isolated from Ganoderma Lucidum Fruiting Bodies. *Food Chem.* 2012, *135*(3), 1097–1103. DOI: 10.1016/j.foodchem.2012.05.071.

[66] Liu, Y.; Huang, G.; Hu, J. Extraction, Characterisation and Antioxidant Activity of Polysaccharides from Chinese Watermelon. *Int. J. Biol. Macromol.* 2018, *111*, 1304–1307. DOI: 10.1016/j.ijbiomac.2018.01.088.

[67] Veselá, A.; Barros, A. S.; Synytsya, A.; Delgadillo, I.; Čopíková, J.; Coimbra, M. A. Infrared Spectroscopy and Outer Product Analysis for Quantification of Fat, Nitrogen, and Moisture of Cocoa Powder. *Analytica Chimica Acta*. 2007, *601*(1), 77–86. DOI: 10.1016/j.aca.2007.08.039.

[68] Li, S.; Shen, Y.; Xie, A.; Yu, X.; Qiu, L.; Zhang, L.; Zhang, Q. Green Synthesis of Silver Nanoparticles Using Capsicum Annuum L. Extract. *Green Chem.* 2007, *9*(8), 852–858. DOI: 10.1039/b615357g.

[69] Pereira, L.; Amado, A. M.; Critchley, A. T.; van de Velde, F.; Ribeiro-Claro, P. J. A. Identification of Selected Seaweed Polysaccharides (Phycocolloids) by Vibrational Spectroscopy (FTIR-ATR and FT-Raman). *Food Hydrocolloids*. 2009, *23*(7), 1903–1909. DOI: 10.1016/j.foodhyd.2008.11.014.

[70] Rahman, M. M.; Al-Sulaimi, S.; Farooque, A. Characterization of New and Fouled SWRO Membranes by ATR/FTIR Spectroscopy. *Appl. Water Sci.* 2018, *8*(6), 1–11. DOI: 10.1007/s13201-018-0806-7.

[71] Liu, X.; Renard, C. M. G. C.; Bureau, S.; Le Bourvellec, C. Revisiting the Contribution of ATR-FTIR Spectroscopy to Characterize Plant Cell Wall Polysaccharides. *Carbohydr. Polym.* 2021, *262*, 117935. DOI: 10.1016/j.carbpol.2021.117935.

[72] Tian, D.; Hu, W.; Zheng, Z.; Liu, H.; Xie, H.-Q. Study on in situ Synthesis of Konjac Glucomannan/Silver Nanocomposites via Photochemical Reduction. *J. Appl. Polym. Sci.* 2006, *100*(2), 1323–1327. DOI: 10.1002/app.23314.

[73] Gautam, V.; Srivastava, A.; Singh, K. P.; Yadav, V. L. Vibrational and gravimetric analysis of polyaniline/polysaccharide composite materials. *Polym. Sci. Ser. A*. 2016, *58*(2), 206–219. DOI: 10.1134/S0965545X16020085.

[74] Samrot, A. V.; Angalene, J. L. A.; Roshini, S. M.; Stefi, S. M.; Preethi, R.; Raji, P.; A, M. K.; Kumar S, S. Purification, Characterization and Exploitation of Azadirachta Indica Gum for the Production of Drug Loaded Nanocarrier. *Mater. Res. Express*. 2020, *7*(5), 055007. DOI: 10.1088/2053-1591/ab8b16.

[75] Li, R.; Chen, W.-C.; Wang, W.-P.; Tian, W.-Y.; Zhang, X.-G. Antioxidant Activity of Astragalus Polysaccharides and Antitumour Activity of the Polysaccharides and SiRNA. *Carbohydr. Polym.* 2010, *82*(2), 240–244. DOI: 10.1016/j.carbpol.2010.02.048.

[76] Chandra, S.; Chatterjee, P.; Dey, P.; Bhattacharya, S. Evaluation of in vitro Anti-Inflammatory Activity of Coffee Against the Denaturation of Protein. *Asian*

Pac. J. Trop. Biomed. 2012, *2*(1), S178–S180. DOI: 10.1016/S2221-1691(12)60154-3.

[77] Gunathilake, K.; Ranaweera, K.; Rupasinghe, H. In vitro Anti-Inflammatory Properties of Selected Green Leafy Vegetables. *Biomedicines*. 2018, *6*(4), 107. DOI: 10.3390/biomedicines6040107.

[78] Ibanoglu, E. Effect of Hydrocolloids on the Thermal Denaturation of Proteins. *Food Chem*. 2005, *90*(4), 621–626. DOI: 10.1016/j.foodchem.2004.04.022.

[79] Yang, L.; Zhang, L.-M. Chemical Structural and Chain Conformational Characterization of Some Bioactive Polysaccharides Isolated from Natural Sources. *Carbohydr. Polym*. 2009, *76*(3), 349–361. DOI: 10.1016/j.carbpol.2008.12.015.

[80] Vidhyalakshmi, R.; Valli, N. C.; Narendra Kumar, G.; Sunkar, S. Bacillus Circulans Exopolysaccharide: Production, Characterization and Bioactivities. *Int. J. Biol. Macromol*. 2016, *87*, 405–414. DOI: 10.1016/j.ijbiomac.2016.02.001.

[81] Middleton, E., Jr; Kandaswami, C. Effects of Flavonoids on Immune and Inflammatory Cell Functions. *Biochem. Pharmacol*. 1992, *43*(6), 1167–1179. DOI: 10.1016/0006-2952(92)90489-6.

[82] Abe, H.; Katada, K.; Orita, M.; Nishikibe, M. Effects of Calcium Antagonists on the Erythrocyte Membrane. *J. Pharm. Pharmacol*. 2011, *43*(1), 22–26. DOI: 10.1111/j.2042-7158.1991.tb05441.x.

[83] Chasis, J. A.; Mohandas, N. Erythrocyte Membrane Deformability and Stability: Two Distinct Membrane Properties That are Independently Regulated by Skeletal Protein Associations. *The J. Cell Biol*. 1986, *103*(2), 343–350. DOI: 10.1083/jcb.103.2.343.

[84] Anosike, C. A.; Obidoa, O.; Ezeanyika, L. U. Membrane Stabilization as a Mechanism of the Anti-Inflammatory Activity of Methanol Extract of Garden Egg (Solanum Aethiopicum). *DARU J. Pharm. Sci*. 2012, *20*(1), 1–7. DOI: 10.1186/2008-2231-20-76.